

Top quark production at the Tevatron

Marc Besançon
CEA-Saclay, DSM/Irfu/SPP
Bat. 141
91191 Gif sur Yvette, France

1 Introduction

The Tevatron is the place of the discovery of the top quark (t) by both the CDF and the D0 experiments [1]. The Tevatron worked extremely well and stopped taking data on September 30th 2011. The Tevatron delivered about 12 fb^{-1} of $p\bar{p}$ collisions and both the CDF and D0 experiments registered more than 10 fb^{-1} of data. The results reported in this mini-review are based on datasets up to 8.7 fb^{-1} . Doing top quark physics means covering a wide spectrum of different subjects including studies of the t (single and pair) production, decay and properties. The present mini-review focuses on results which were available at the time of the 2012 FPCP conference on the measurements of the $t\bar{t}$ cross section, the forward backward asymmetry, the spin correlations and the ratio of branching fractions as well as on single t cross section and $|V_{tb}|$ measurements. We will also report on recent searches for new resonances with $t\bar{t}$ final states. At the Tevatron, within the Standard Model (SM), $t\bar{t}$ production is expected to occur via strong interactions namely through $q\bar{q}$ annihilation (85%) and gluon gluon (gg) fusion (15%). Typical next-to-leading (NLO) predictions amount to $\sigma_{NLO}(p\bar{p} \rightarrow t\bar{t}) = 7.46_{-0.67}^{+0.48} \text{ pb}$ for $m_t = 172.5 \text{ GeV}$ [2] and for NNLO $\sigma_{NNLO}(p\bar{p} \rightarrow t\bar{t}) = 7.067_{-0.232}^{+0.143} \text{ (scales)}_{-0.122}^{+0.186} \text{ (pdf)} \text{ pb}$. for $m_t = 173.3 \text{ GeV}$ [3]. On the other hand, single t production is expected to occur via electroweak interactions either in the s-channel (33 %) or the t-channel (67 %) with the following SM predictions for the cross sections $\sigma^{s\text{-channel}} = 1.05 \pm 0.07 \text{ pb}$ and $\sigma^{t\text{-channel}} = 2.10 \pm 0.19 \text{ pb}$ for $m_t = 172.5 \text{ GeV}$ [4]. The single t associated production Wt having a production cross section of the order of 0.2 pb is too small at the Tevatron. The t decays before it hadronizes. The t decays into a b quark and an on-shell W gauge boson ($t \rightarrow Wb$) with a branching ratio close to 1. The final states corresponding to $t\bar{t}$ production are classified according to the decay of the W gauge boson from the parent t . The results reported here concentrate on the lepton+jets channels where one W gauge boson decays leptonically i.e. $W \rightarrow l\nu$ where $l = \mu$ or e (amounting to 30% of all the $t\bar{t}$ channels) and dilepton channels where both W decay leptonically (5%). Other channels include all hadronic channels where both W gauge bosons decay hadronically

($W \rightarrow qq'$, 45%) as well as tauonic channels where both W decay leptonically into tau leptons (20%). Bottom quarks are always present in the final state and we can use b-quark identification techniques to help for the selection of top quark events.

2 top quark pair production

The top quark is a unique particle. It is the heaviest of all known particle and it decays before hadronizing. Studying $t\bar{t}$ production provides a very good test of the SM. Furthermore the measurement of the cross section is the first step in understanding any selected $t\bar{t}$ sample. If physics beyond the SM exists, it can change the overall production rate or the rate in different channels. Finally top quark pair production is also a background for searches for new physics.

2.1 Cross section measurements

The most precise measurement of the $t\bar{t}$ production cross section at the Tevatron is obtained in the lepton+jets channels. Both CDF and D0 have performed measurements based on kinematical approaches and b-quark jet tagging. The CDF kinematical approach uses pre-tagged samples and a neural network discriminant. CDF measures the ratio $\sigma_{t\bar{t}}/\sigma_{Z/\gamma^* \rightarrow l+l^-}$ of the $t\bar{t}$ cross section and the Z boson production cross section which allows to reduce the systematic uncertainties from luminosity. By using the theoretical value for σ_{Z/γ^*} , one can extract the $t\bar{t}$ cross section. Combining this approach with b-quark jet tagging, CDF finds $\sigma_{t\bar{t}} = 7.70 \pm 0.52$ (stat+syst) pb using a dataset of 4.3 fb^{-1} and assuming $m_t = 172.5 \text{ GeV}$ [5]. From a combination of a kinematical approach and b-quark jet tagging D0 determines the $t\bar{t}$ production cross section and the background from W boson + heavy or light flavor production simultaneously. D0 finds $\sigma_{t\bar{t}} = 7.78 \pm 0.25$ (stat) $^{+0.73}_{-0.59}$ (syst) pb using a dataset of 5.3 fb^{-1} and assuming $m_t = 172.5 \text{ GeV}$ [6]. The dominant systematic uncertainties are coming from jet energy scale, b-quark jet tagging acceptances, and the estimation of the W+b background. All measurement are now dominated by systematic uncertainties. Combining all their measurement channels, CDF finds $\sigma_{t\bar{t}} = 7.50 \pm 0.48$ (stat+syst) pb i.e. a precision of 6.4 %, with datasets up to 5.7 fb^{-1} . The results are in agreement with the predictions of the SM and are consistent across channels, methods and experiments.

2.2 Forward backward asymmetry

At the Tevatron the $t\bar{t}$ production is predicted to be charge symmetric at LO in QCD. However NLO calculations predicts asymmetries in the 5%-10% range [7] and next-to-next-to-leading order (NNLO) calculations predict significant corrections for $t\bar{t}$ production in association with a jet [8]. The charge asymmetry arises from interferences between symmetric and antisymmetric contributions under the exchange $t \leftrightarrow \bar{t}$.

The charge asymmetry depends on the region of phase space and, in particular, on the production of an additional jet. Tree level and box diagrams interferences give a positive asymmetry while initial and final state radiation interferences give a negative asymmetry. The small asymmetries expected in the SM makes this a sensitive probe for new physics [9].

Experimentally the t direction and rapidity, defined as function of the polar angle θ and the ratio of the particle's momentum to its energy β as $y(\theta, \beta) = \frac{1}{2} \ln[(1 + \beta \cos\theta)/(1 - \beta \cos\theta)]$, are reconstructed and the rapidity difference $\Delta y = y_t - y_{\bar{t}}$ is used. The background is then subtracted from data. CDF estimates the background from Monte Carlo (MC) simulations. For D0 the background is fitted with likelihood discriminants.

The raw asymmetry

$$A_{fb} = \frac{N(\Delta y > 0) - N(\Delta y < 0)}{N(\Delta y > 0) + N(\Delta y < 0)}, \quad (1)$$

where $N(\Delta y > 0)$ ($N(\Delta y < 0)$) is the number of event with positive (negative) Δy , is then extracted. The next step consists in performing unfolding i.e. correcting the raw asymmetry for acceptance and resolution back to production level.

Using a dataset of about 5 fb^{-1} both CDF and D0 find that inclusive asymmetries exceed the SM prediction by 1.5 to 2 standard deviation [11, 12] with an unclear dependence on the invariant mass of the $t\bar{t}$ system i.e. $M_{t\bar{t}}$, and Δy . Remarkably enough CDF finds an asymmetry which is about 3 standard deviations away from the prediction of MC@NLO [10] for $M_{t\bar{t}} > 450 \text{ GeV}$ [11].

CDF updated recently its forward backward asymmetry measurement with the full datasets 8.7 fb^{-1} in the lepton+jets channels and using POWHEG [13] (with electroweak corrections) for the SM predictions.

Fig. 1 shows the Δy distribution from CDF after background subtraction and unfolding. CDF finds an inclusive asymmetry [14]:

$$A_{fb} = 0.162 \pm 0.041(stat) \pm 0.022(syst) \quad (2)$$

which is compatible with their previous measurement with a smaller dataset. In the SM the forward backward asymmetry is expected to increase with $M_{t\bar{t}}$ and with Δy [15]. Beyond SM physics could show different dependences than in the SM. As can be seen from Fig. 2 the $M_{t\bar{t}}$ dependency is well fit with a linear function. The same holds for the Δy dependence [14].

Tab.1 shows the values of the slope parameter of the best linear fit for the dependences of A_{FB} on $M_{t\bar{t}}$ and Δy for both data and SM predictions.

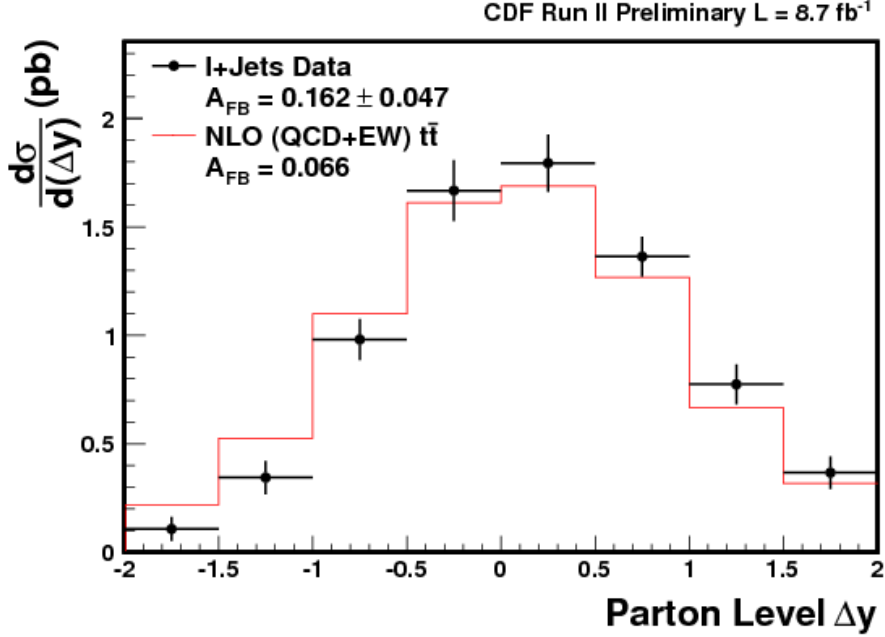


Figure 1: Δy distribution from CDF after background subtraction and unfolding (from [14]).

2.3 Spin correlations

Top quark pairs are produced with a definite spin state depending on the production mechanism i.e. spin 1 for $q\bar{q}$ annihilation and spin 0 for gluon fusion. Since t decays before hadronizing the spin information is expected to pass to the decay products. The spin correlation from t decay products can be measured from the angular distribution

$$\frac{1}{\sigma} \frac{d^2\sigma}{d\cos\theta_1 d\cos\theta_2} = \frac{1}{4}(1 - C\cos\theta_1\cos\theta_2) \quad (3)$$

where θ_1 and θ_2 denote the angles between the direction of flight of the decay leptons (for leptonically decaying W bosons) or jets (for hadronically decaying W bosons) in

slope parameter	A_{FB} vs $M_{t\bar{t}}$	A_{FB} vs Δy
DATA	$(15.6 \pm 5.0) \times 10^{-4}$	$(30.6 \pm 8.6) \times 10^{-2}$
SM	3.3×10^{-4}	10.3×10^{-2}

Table 1: CDF $t\bar{t}$ forward backward asymmetry as a function of $M_{t\bar{t}}$ and Δy : best fit slope for observed data compared to NLO prediction (from [14]).

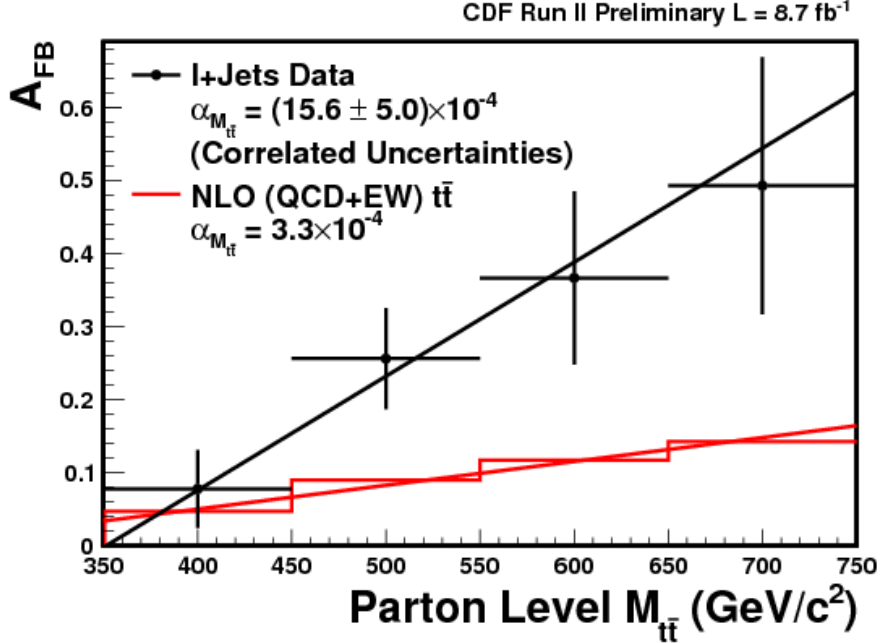


Figure 2: A_{FB} as a function of $M_{t\bar{t}}$ from CDF data with a dataset of 8.7 fb⁻¹ (from [14]).

the parent t and \bar{t} rest frames and the spin quantization axis, and introducing the correlation strength C :

$$C = \frac{N_{\uparrow\uparrow} + N_{\downarrow\downarrow} - N_{\uparrow\downarrow} - N_{\downarrow\uparrow}}{N_{\uparrow\uparrow} + N_{\downarrow\downarrow} + N_{\uparrow\downarrow} + N_{\downarrow\uparrow}} \quad (4)$$

where $N_{\uparrow\uparrow}$ ($N_{\uparrow\downarrow}$ etc...) is the number of $t\bar{t}$ pairs with the spins parallel (or anti-parallel etc...) to a certain basis. In the beam momentum vector as the spin quantization axis, the NLO SM prediction for the correlation strength is $C = 0.777^{+0.027}_{-0.042}$ [16].

At the Tevatron the spin correlations are measured using templates with different C values. The templates are then compared with data using maximum likelihood fits. Using datasets of 5.1 and 5.4 fb⁻¹ respectively, CDF finds $C = 0.04 \pm 0.56$ (stat+syst) [17] and D0 finds $C = 0.10 \pm 0.45$ (stat+syst) [18] both in the dilepton channel. In the lepton+jets and using a dataset of 5.3 fb⁻¹ CDF finds $C = 0.72 \pm 0.69$ (stat+syst) [19]. The results are consistent with SM expectations but are limited by statistical uncertainties.

The D0 experiment has developed an alternate method based on the so called matrix element method where an event probability can be defined from the differential cross section of the $t\bar{t}$ production process $\sigma(y, H)$, the detector response $W(x, y)$

that describes the probability of a partonic final state y to be measured as x and the parton density functions together with the correlation ($H=1$) and no correlation ($H=0$) hypotheses [20]:

$$P(x, H) \sim \int d^6\sigma(y, H)W(x, y)f_{PDF}(q_1)f_{PDF}(q_2)dq_1dq_2. \quad (5)$$

One can build a discriminating variable R from these probabilities:

$$R = \frac{P(x, H = 1)}{P(x, H = 1) + P(x, H = 0)}. \quad (6)$$

Fig. 3 shows the distribution of the discriminant variable R from D0 in the lepton+jets channel using a dataset of 5.3 fb^{-1} [20]. A binned maximum likelihood fit to the R distribution is performed to extract the correlation strength. D0 finds $C^{dil} = 0.57 \pm 0.31$ (stat+syst) in the dileptons channels and $C^{l+jets} = 0.89 \pm 0.33$ (stat+syst) in the lepton+jets channels using datasets of 5.3 and 5.4 fb^{-1} respectively.

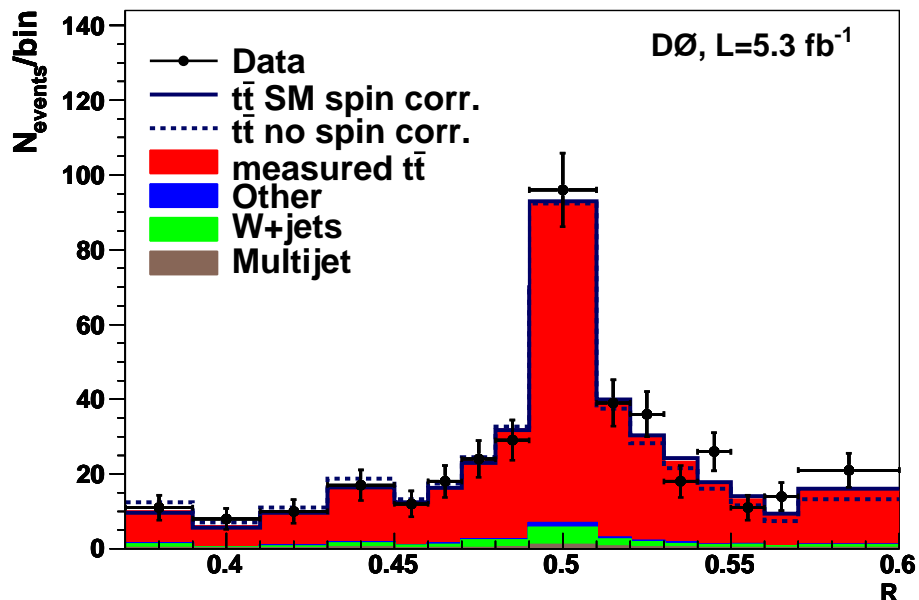


Figure 3: D0 discriminating variable R (see text) for the $t\bar{t}$ spin correlations measurements with the matrix element method (from [20]).

Combining the lepton+jets and the dilepton channels allows the D0 experiment to find $C = 0.66 \pm 0.23$ (stat+syst) and $C > 0.26$ at 95 % of confidence limit as well as exclude the $C=0$ hypothesis at the level of 3.1 standard deviations. This is the first evidence of non zero spin correlation in $t\bar{t}$ production [20].

2.4 Ratio of branching ratios

In the SM the ratio of branching fractions defined by:

$$R_b = \frac{BR(t \rightarrow Wb)}{BR(t \rightarrow Wq)} = \frac{|V_{tb}|^2}{|V_{td}|^2 + |V_{ts}|^2 + |V_{tb}|^2} \quad (7)$$

is constrained by the unitarity of the CKM matrix to be equal to 1. Any value below 1 could indicate new physics. One can drop the assumption $R = 1$ in the $t\bar{t}$ cross section measurements. This has been done by the D0 experiment for the dilepton and lepton+jets channels using a dataset of 5.4 fb^{-1} [22] and by the CDF experiment in the lepton+jets channels using a dataset of 8.7 fb^{-1} [21]. The measurement of CDF is based on the determination of the number of b-quark jets in $t\bar{t}$ events using lepton+jets samples i.e. samples with at least 3 jets in the final state further divided into subsets according to the lepton type, jet multiplicity and number of b-tagged jets. The comparison between the prediction and the observed data in each subsample is made by using a likelihood function where R_b and the $t\bar{t}$ production cross section are simultaneously fit. CDF measures $R = 0.94 \pm 0.09$ (stat+syst) and $\sigma_{t\bar{t}} = 7.5 \pm 1.0$ (stat+syst) pb. Assuming the unitarity of the CKM matrix and 3 generations of quarks one can extract $V_{tb} = 0.97 \pm 0.05$ (stat+syst). Using a dataset of 5.4 fb^{-1} and combining the lepton+jets and the dilepton channels, the D0 experiment measures [22] $R = 0.90 \pm 0.04$ (stat+syst), $\sigma_{t\bar{t}} = 7.74_{-0.57}^{+0.67}$ (stat+syst) pb. Assuming the unitarity of the CKM matrix and 3 generations of quarks, D0 extracts $V_{tb} = 0.95 \pm 0.02$ (stat+syst) and $V_{tb} > 0.88$ at 95% confidence level. As we will see in the next section, V_{tb} can be directly measured from the measurement of the single t production cross section.

3 single top quark production

Single t production via electroweak interactions has been observed for the first time by the CDF and DO experiments in march 2009 [23]. As mentioned above, single t production is expected to occur via electroweak interactions either in the s-channel (33 %) or the t-channel (67 %) with the following SM predictions for the cross sections $\sigma^{s\text{-channel}} = 1.05 \pm 0.07$ pb and $\sigma^{t\text{-channel}} = 2.10 \pm 0.19$ pb for $m_t = 172.5$ GeV [4]. The single t associated production Wt having a production cross section of the order of 0.2 pb is too small at the Tevatron. Single t production measurement allows for a direct access to the W-t-b vertex and thus to a direct measurement of the V_{tb} matrix element of the CKM matrix. One of the major difficulty with single t production measurements comes from the fact that there is a large background with uncertainties larger than the single t signal itself. As a consequence, the use of multivariate techniques (MVA) are mandatory and several of them are used such as boosted decision

trees [24] (BDT), bayesian neural network [25] (BNN), neuroevolution of augmented topologies [26] (NEAT).

Using a dataset corresponding to an integrated luminosity of up to 3.2 fb^{-1} the combination of Tevatron results gives [27] $\sigma_{single-top} = 2.76_{-0.47}^{+0.58}$ (stat+syst) for $m_t = 170 \text{ GeV}$, $V_{tb} = 0.88 \pm 0.07$ (stat+syst) and $V_{tb} > 0.77$ at 95% confidence level. These measurements have been updated with larger datasets and, in the following, we are going to summarize these new results.

3.1 Cross section and V_{tb} measurements

The D0 experiment has updated its results in the lepton+jets channel [28] where the W boson from the parent t is decaying leptonically (electron and muon are the lepton flavors under consideration) and this with a dataset of 5.4 fb^{-1} . The discriminating variables (single object kinematics, global event kinematics, jet reconstruction, t reconstruction and angular correlations) allowing to separate the signal from the background are combined into various MVAs i.e. BDT, BNN and NEAT. The MVAs are trained separately for the two single t production channels namely the s-channel (tb) production considered as the signal and the t-channel (tbq) production as part of the background on the one hand and vice and versa on the other hand. The correlation among the outputs of the individual MVA is about 70%. A second BNN is used to construct a combined discriminant for each channel. A bayesian approach is then used to extract the production cross section. The method consists of forming binned likelihood as a product of the six analysis channels built from the jet multiplicities i.e. 2, 3 or 4 jets with 1 or 2 b-tagged jets and bins using the full discriminant outputs. Poisson distribution for the number of events in each bin as well as uniform prior probabilities for non-negative values of the signal cross sections are assumed. Systematic uncertainties and their correlations are taken into account assuming a Gaussian prior for each source of systematic uncertainty. The production cross section is then given by the position of the maximum of a posterior probability density function of single t cross section. The D0 experiment finds $\sigma_{s+t} = 3.43_{-0.74}^{+0.73}$ pb, $\sigma_{t-channel} = 2.86_{-0.63}^{+0.69}$ pb and $\sigma_{s-channel} = 3.43_{-0.35}^{+0.38}$ pb with combined statistical and systematic uncertainties.

This measurement allows for a direct measurement of the V_{tb} matrix element of the CKM matrix as the single t production cross section is directly proportional to $|V_{tb}|^2$. One can measure V_{tb} assuming V-A couplings but without assuming 3 generations or the unitarity of the CKM matrix. One can also maintain the possibility for an anomalous strength of the left handed W-t-b coupling f_1^L which would rescale the single t cross section [29]. From a bayesian analysis the D0 experiment finds $|V_{tb}f_1^L| = 1.02_{-0.11}^{+0.10}$. Assuming $f_1^L = 1$ and restricting the prior to the $[0,1]$ interval one finds $V_{tb} > 0.79$ at the 95% confidence level.

The D0 experiment has also performed a model independent measurement of t-channel and s-channel single t cross sections production. Following the approach

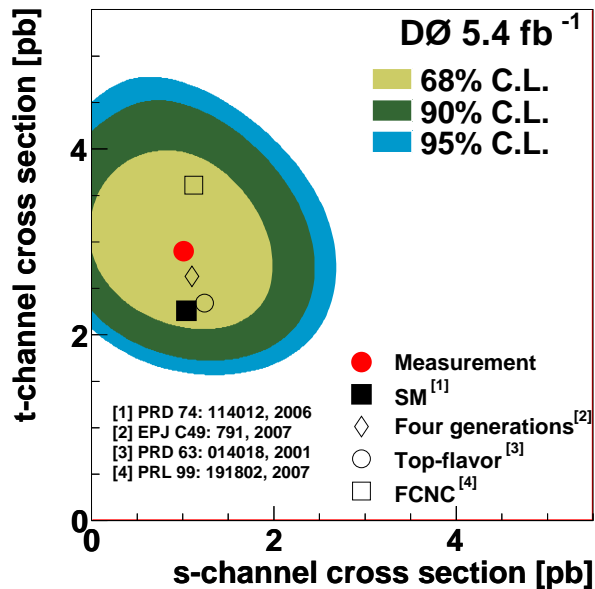


Figure 4: Posterior probability density for the t-channel vs s-channel single t production in contours of equal probability density (from [30]).

of [30] and using the method described above, one can construct a two-dimensional posterior probability density function as a function of the cross sections of the t- and s-channel processes. Fig. 4 shows the posterior probability density for the t-channel vs s-channel single t production in contours of equal probability density. The t-channel cross section is then extracted from a one-dimensional posterior probability density function by integrating the previous two-dimensional probability density function over the s-channel cross section axis thus making no assumptions about the value of the s-channel cross section. One can similarly extract the s-channel cross section by integrating the two-dimensional probability density function over the t-channel cross section axis. With a dataset of 5.4 fb^{-1} DØ finds $\sigma_{t\text{-channel}} = 2.90 \pm 0.59 \text{ pb}$ and $\sigma_{s\text{-channel}} = 0.98 \pm 0.63 \text{ pb}$, statistical and systematic uncertainties being combined. This gives the most precise cross sections measurement in the t-channel with a significance bigger than 5 standard deviations.

The CDF experiment has also updated its single-top measurements in the lepton+jets channel using a dataset of 7.5 fb^{-1} [32]. CDF uses a neural network discriminant with the same input variables as the observation analysis. CDF uses now the NLO POWHEG program for the simulation of the single t signal. Fig. 5 shows the neural network discriminant distribution.

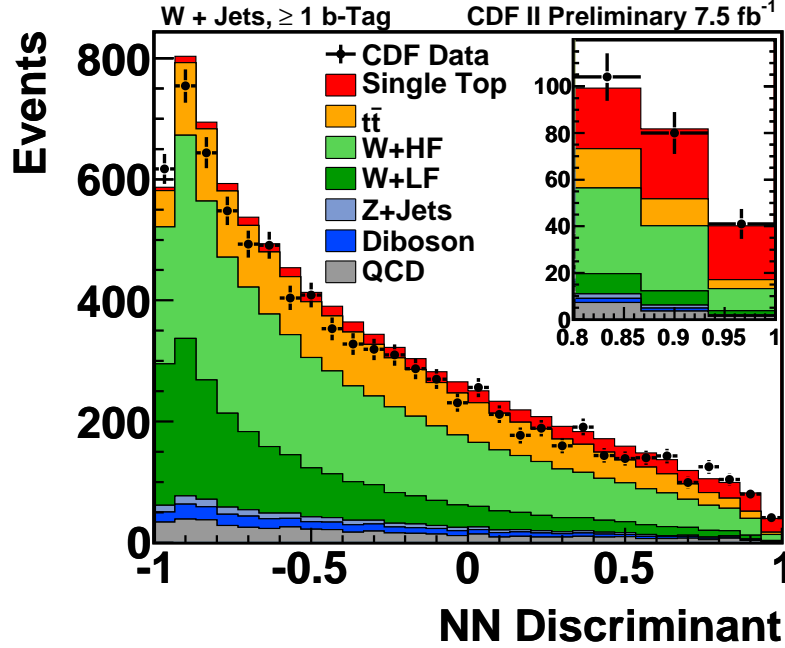


Figure 5: CDF neural network output for the single t production cross section measurement with the 7.5 fb^{-1} dataset (from [32]).

CDF finds $\sigma_{\text{single-top}} = 3.04^{+0.57}_{-0.53}$ pb for $m_t = 172.5$ GeV. Using:

$$|V_{tb}|_{\text{measured}}^2 = \frac{\sigma_{s+t}^{\text{measured}}}{\sigma_{s+t}^{\text{SM}}} |V_{tb}|_{\text{SM}}^2 \quad (8)$$

where $|V_{tb}|_{\text{SM}}^2 \approx 1$. CDF extracts $V_{tb} = 0.96 \pm 0.09$ (stat+syst) ± 0.05 (theory) and sets $V_{tb} > 0.78$ at 95% confidence level.

4 Search for new physics with top quark

Many searches for physics beyond the SM can be performed with $t\bar{t}$ final states at the Tevatron. In particular searches for new resonances decaying into $t\bar{t}$ allows to explore many theories beyond the SM.

Both the CDF and D0 experiments looked for a resonant $t\bar{t}$ production in the lepton+jets channels.

CDF examined the $t\bar{t}$ invariant mass spectrum of candidate events where the event kinematics have been reconstructed applying the matrix element method for SM $t\bar{t}$ production and decay. The observed $t\bar{t}$ invariant mass spectrum is then compared to

templates models of signal such as heavy vector boson decaying into $t\bar{t}$ ($Z' \rightarrow t\bar{t}$) and background processes in an unbinned maximum likelihood fit. One can then constrain the $Z' \rightarrow t\bar{t}$ cross section times branching ratio. Using a dataset of 4.8 fb^{-1} CDF data indicate no evidence of resonant production of $t\bar{t}$. CDF excludes a benchmark model of leptophobic $Z' \rightarrow t\bar{t}$ with $m_{Z'} < 900 \text{ GeV}$ at 95% confidence level [33].

In the case of the D0 experiment, the $t\bar{t}$ invariant mass spectrum is reconstructed from the event kinematics. In this approach the momentum of the neutrino is determined by equating the neutrino transverse momentum to the measured missing transverse momentum of the event constraining the invariant mass of the charged lepton-neutrino system to the W boson mass and choosing the smaller solution of the resulting quadratic equation for the neutrino momentum longitudinal component along the beam direction. The reconstructed invariant $t\bar{t}$ mass is used to test for the presence of a signal in the data and to set constraints on the production cross section of a narrow $t\bar{t}$ resonance times branching fraction to $t\bar{t}$ as a function of its mass. Using a dataset of 5.3 fb^{-1} D0 data indicate no evidence of resonant production of $t\bar{t}$. D0 excludes a benchmark model of leptophobic $Z' \rightarrow t\bar{t}$ with $m_{Z'} < 835 \text{ GeV}$ at 95% confidence level [34].

As mentioned in section 2.2, CDF results on the $t\bar{t}$ forward backward asymmetry A_{FB} indicate a discrepancy with current SM predictions. A wide class of models have been built to explain such a discrepancy involving the production of a new heavy particle enhancing A_{FB} . This new heavy particle can also be singly produced in association with a top quark (or anti-top quark) and further decay into an anti-top quark and an additional quark (or top quark and an additional quark) looking like a t +jet resonance in $t\bar{t}$ + jet events. Using a dataset of 8.7 fb^{-1} , CDF has performed a search for such events using the lepton+jets channel with at least 5 jets and at least one b-tagged jet. CDF finds the data to be consistent with the SM prediction and sets cross section upper limits from 0.61 pb to 0.02 pb for resonances ranging from 200 GeV to 800 GeV [35].

5 Summary

The CDF and D0 experiments at the Tevatron provide precision measurements for $t\bar{t}$ production cross section. In most cases the measurements are now limited by systematic uncertainties. Forward backward asymmetry of top events keeps indicating a discrepancy with current NLO QCD prediction. The Tevatron provides the first evidence for non zero spin correlations in $t\bar{t}$ events. New results on the measurement of single t production cross sections reach precisions better than 20%. The production via the t-channel process has been observed. Measurements and limits on the matrix element V_{tb} of the CKM matrix have been provided. Finally there is no evidence for resonant $t\bar{t}$ production in CDF and D0 data and constraints have been set on

benchmark models such as leptophobic Z' .

References

- [1] CDF collaboration, F. Abe *et al.*, *Phys. Rev. Lett.* **74**, 2626 (1995); D0 collaboration, S. Abachi *et al.*, *Phys. Rev. Lett.* **74**, 2632 (1995).
- [2] S. Moch and P. Uwer, PRD **78**, 034003 (2008).
- [3] P. Bernreuther, M. Czakon, A. Mitov, arXiv:1204.5201.
- [4] N. Kidonakis, PRD **81**, 054028 (2010) and PRD **83**, 091503 (2011).
- [5] CDF Collaboration, T. Aaltonen *et al.*, *Phys. Rev. Lett.* **105**, 012001 (2010).
- [6] D0 Collaboration, V. M. Abazov *et al.*, *Phys. Rev. D* **84**, 012008 (2011).
- [7] J. H. Kühn and G. Rodrigo, *Phys. Rev. Lett.* **81**, 49 (1998); J. H. Kühn and G. Rodrigo, *Phys. Rev. D* **59**, 054017 (1999); M. T. Bowen *et al.*, *Phys. Rev. D* **73**, 14008 (2006).
- [8] S. Dittmaier, P. Uwer and S. Weinzierl, *Phys. Rev. Lett.* **98**, 262002 (2007).
- [9] J.A. Aguilar-Saavedra, arXiv:1202.2382.
- [10] S. Frixione and B. R. Webber, JHEP **0206**, 029 (2002); S. Frixione, P. Nason and B. R. Webber, JHEP **0308**, 007 (2003) ; S. Frixione, E. Laenen, P. Motylinski and B. R. Webber, JHEP **0603** 092 (2006) ; S. Frixione, E. Laenen, P. Motylinski, B. R. Webber and C. D. White, JHEP **0807** 029 (2008) ; S. Frixione, F. Stoeckli P. Torrielli and B. R. Webber, JHEP **1101** 053 (2011).
- [11] CDF Collaboration, T. Aaltonen *et al.*, *Phys. Rev. D* **83**, 112003 (2011) ; Conference notes 10436 and 10584.
- [12] D0 Collaboration, V. M. Abazov *et al.*, *Phys. Rev. D* **84**, 112055 (2011).
- [13] S. Frixione, G. Ridolfi and P. Nason, JHEP **0709**, 126 (2007) ; W. Hollik and D. Pagani, PRD **84**, 093003 (2011) ; J. H. Kühn and G. Rodrigo, JHEP **1201**, 063 (2012) ; A. V. Manohar and M. Trott, PLB **711**, 313 (2012).
- [14] CDF Collaboration, Conference Note 10807.
- [15] L. G. Almeida, G. Sterman and W. Vogelsang, PRD **78**, 014008 (2008) ; M. Gresham, I. W. Kim and K. Zurek, PRD **83**, 114027 (2011).

- [16] W. Bernreuther, A. Brandenburg, Z. G. Si, P. Uwer, *Nucl. Phys. B* **690**, 81 (2004).
- [17] CDF Collaboration, CDF Conference note 10719.
- [18] D0 Collaboration, V. M. Abazov *et al.*, *Phys. Lett. B* **702**, 16 (2011).
- [19] CDF Collaboration, CDF Conference note 10211.
- [20] D0 Collaboration, V. M. Abazov *et al.*, *Phys. Rev. Lett.* **108**, 032004 (2012).
- [21] Using the CDF Conference note 10887 (dated June 19th) with publication time June 30th according to the CDF public website i.e. after the time of the FPCP 2012 conference. The actual review talk has been based on the talks from S. Leone and D. Mietlicki at Rencontres de Moriond 2012 using a dataset of 7.5 fb^{-1} .
- [22] D0 Collaboration, V. M. Abazov *et al.*, *Phys. Rev. Lett.* **107**, 121802 (2011).
- [23] D0 Collaboration, V. M. Abazov *et al.*, *Phys. Rev. Lett.* **103**, 092001 (2009) ; CDF Collaboration, T. Aaltonen *et al.*, *Phys. Rev. Lett.* **103**, 092002 (2009).
- [24] L. Breiman *et al.*, Classification and Regression Trees, Wadsworth, Stamford, 1984.
- [25] R. M. Neal, Bayesian Learning for Neural Networks, Springer-Verlag, New York, 1996.
- [26] K. O. Stanley and R. Miikkulainen, Evolutionary Computation **10**, 99 (2002).
- [27] CDF and D0 combinations arXiv:0908.2171.
- [28] D0 Collaboration, V. M. Abazov *et al.*, *Phys. Rev. D* **84**, 112001 (2011).
- [29] G. L. Kane, G. A. Ladinsky and C. P. Yuan, PRD **45**, 124 (1992).
- [30] D0 Collaboration, V. M. Abazov *et al.*, *Phys. Lett. B* **682**, 363 (2010).
- [31] D0 Collaboration, V. M. Abazov *et al.*, *Phys. Lett. B* **705**, 313 (2011).
- [32] CDF Collaboration, Conference note 10793.
- [33] CDF Collaboration, T. Aaltonen *et al.*, *Phys. Rev. D* **84**, 072004 (2011).
- [34] D0 Collaboration, V. M. Abazov *et al.*, *Phys. Rev. D* **85**, 051101 (2012).
- [35] CDF Collaboration, Conference note 10776.